



저작자표시-비영리-변경금지 2.0 대한민국

이용자는 아래의 조건을 따르는 경우에 한하여 자유롭게

- 이 저작물을 복제, 배포, 전송, 전시, 공연 및 방송할 수 있습니다.

다음과 같은 조건을 따라야 합니다:



저작자표시. 귀하는 원저작자를 표시하여야 합니다.



비영리. 귀하는 이 저작물을 영리 목적으로 이용할 수 없습니다.



변경금지. 귀하는 이 저작물을 개작, 변형 또는 가공할 수 없습니다.

- 귀하는, 이 저작물의 재이용이나 배포의 경우, 이 저작물에 적용된 이용허락조건을 명확하게 나타내어야 합니다.
- 저작권자로부터 별도의 허가를 받으면 이러한 조건들은 적용되지 않습니다.

저작권법에 따른 이용자의 권리는 위의 내용에 의하여 영향을 받지 않습니다.

이것은 [이용허락규약\(Legal Code\)](#)을 이해하기 쉽게 요약한 것입니다.

[Disclaimer](#)

c-Met-mediated reactivation of
PI3K/AKT signaling contributes to
insensitivity of BRAF(V600E) mutant
thyroid cancer to BRAF inhibition



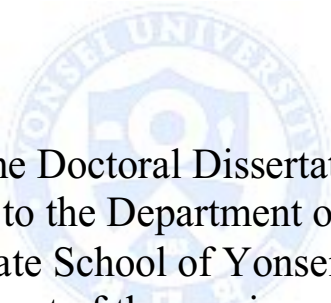
Hyung Kwon Byeon

Department of Medicine

The Graduate School, Yonsei University

c-Met-mediated reactivation of
PI3K/AKT signaling contributes to
insensitivity of BRAF(V600E) mutant
thyroid cancer to BRAF inhibition

Directed by Professor Eun Chang Choi



The Doctoral Dissertation
submitted to the Department of Medicine,
the Graduate School of Yonsei University
in partial fulfillment of the requirements for the degree
of Doctor of Philosophy

Hyung Kwon Byeon

June 2015

This certifies that the Doctoral
Dissertation of Hyung Kwon Byeon
is approved.

Thesis Supervisor : Eun Chang Choi

Thesis Committee Member#1 : Yoon Woo Koh

Thesis Committee Member#2 : Chul-Ho Kim

Thesis Committee Member#3: Nam Hoon Cho

Thesis Committee Member#4: Ho-Geun Yoon

The Graduate School
Yonsei University

June 2015

ACKNOWLEDGEMENTS

First of all, I would like to express my deepest gratitude towards my mentor, Professor Eun Chang Choi, for his enthusiasm and passion towards his pupil. He has guided me all the way and taught me in every aspects of my life to become what I am now today.

Next, I am obliged to pass my most sincere appreciation to Professor Yoon Woo Koh, who has provided every help to put all this together. His dedication and effort to enlighten me in the basic scientific research will be treasured indefinitely and will be the fundamental motivation of my academic career.

Truly thanks to Professors Chul-Ho Kim, Nam Hoon Cho, and Ho-Geun Yoon who have spared no pains in giving critical advice for improvement of the quality of this study, in spite of their busy schedule.

Lastly, the greatest acknowledgement goes to my lifetime companion, my loving wife. For without her kind understanding and unfathomed support in every ways, this Dissertation could never see the light of day.

<TABLE OF CONTENTS>

ABSTRACT	1
I. INTRODUCTION	3
II. MATERIALS AND METHODS	7
1. Cell Culture	7
2. Confirmation of c-Met expression and c-Met inhibitor-induced suppression of c-Met expression by Western blot analysis	7
3. Cell proliferation assay	8
4. Immunohistochemical analysis	9
5. FACScan with Annexin V-fluorescein isothiocyanate (FITC) / propidium iodide (PI) staining	9
6. Orthotopic xenograft mouse model	10
7. Terminal deoxynucleotidyltransferase-mediated dUTP-biotin nick end labeling (TUNEL) assay	10
8. Immunofluorescence	11
9. Pathscan RTK signaling antibody array	11
10. Hepatocyte growth factor (HGF) ELISA	12
11. Transient transfection of c-Met and RNA interference (siRNA)	12
12. Statistical analysis	13
III. RESULTS	13
1. PLX4032 shows different drug sensitivity against different BRAF (V600E) mutant thyroid cancer cell lines	13
2. PLX4032 induces over-expression of p-c-Met and subsequently over-expression of PI3K / AKT pathway in BRAF (V600E) mutant anaplastic thyroid cancer cell (8505C)	17

3. Inhibition of c-Met can reverse the over-expression of PI3K / AKT pathway after treatment of PLX4032 in BRAF (V600E) mutant anaplastic thyroid cancer cell (8505C)	22
4. PLX4032 induces the expression of HGF in BRAF (V600E) mutant anaplastic thyroid cancer cell (8505C)	26
5. Combinatorial treatment of PLX4032 and PHA665752 can inhibit the tumor growth in an orthotopic xenograft mouse model	28
IV. DISCUSSION	35
V. CONCLUSION	40
REFERENCES	41
ABSTRACT (IN KOREAN)	45
PUBLICATION LIST	47



LIST OF FIGURES

Figure 1. Differential drug sensitivity of BRAF (V600E) mutant thyroid cancer cell lines 8505C and BCPAP to PLX4032 treatment	14
Figure 2. Western blot analysis after treatment with PLX4032 of increasing treatment times	15
Figure 3. Analysis of apoptotic cell death with Annexin V-FITC/PI staining	15
Figure 4. TUNEL assay after PLX4032 treatment	16
Figure 5. MTT assay done after treatment with PLX4032 until 48 hours in 8505C cells	17
Figure 6. RTK array after treatment with PLX4032 for 9 hours in 8505C cells	18
Figure 7. Western blot analysis after treatment of PLX4032 for 3 and 6 hours in both 8505C and BCPAP cells	19
Figure 8. Western blot analysis after treatment of PLX4032 of increasing dosages for 3 hours in 8505C cells	20
Figure 9. Western blot analysis after treatment of PLX4032 of increasing treatment times in 8505C cells	21
Figure 10. 8505C cells transfected with c-Met small interfering RNA (siRNA) or negative control siRNA treated with PLX4032 for 3,6, and 9 hours	22

Figure 11. Western blot analysis of each after treatment of PLX4032 and dual treatment of PLX4032 and PHA665752 for 3 and 6 hours in 8505C cells	23
Figure 12. Western blot analysis after treatment of PHA665752 for 3,6, and 9 hours in 8505C cells	24
Figure 13. MTT assay done after different drug treatment conditions for 24 hours in 8505C cells	24
Figure 14. TUNEL assay of 8505C cells treated under different drug regimens.	25
Figure 15. Western blot analysis of each after treatment of PLX4032 and dual treatment of PLX4032 and PHA665752 in 8505C cells	26
Figure 16. HGF ELISA after PLX4032 treatment of increasing duration in 8505C and BCPAP cells	27
Figure 17. Western blot analysis after treatment of PLX4032 for 3,6, and 9 hours in 8505C cells	27
Figure 18. Western blot analysis after different treatment conditions consisting of PLX4032, PHA665752, and HGF for 9 hours in 8505C cells	28
Figure 19. Treatment response to PLX4032 and PHA665752 in a xenograft mouse model orthotopically injected with 8505C cells	29
Figure 20. Assessment of tumor volume and weight 3 weeks following different drug treatments in orthotopic xenograft mouse model.....	31

Figure 21. Western blot analysis of intratumoral protein expression after drug treatment in tumor specimens of 8505C cells orthotopically-injected mice 32

Figure 22. Histopathological analysis confirmed by H & E staining from tumor tissue samples derived from mice of each group with different drug treatment conditions 34

Figure 23. Immunohistochemistry evaluation of tumor tissues from each treatment group 35



ABSTRACT

c-Met-mediated reactivation of PI3K/AKT signaling contributes to insensitivity of BRAF(V600E) mutant thyroid cancer to BRAF inhibition

Hyung Kwon Byeon

*Department of Medicine
The Graduate School, Yonsei University*

(Directed by Professor Eun Chang Choi)

BRAF (V600E) mutation is the most commonly detected genetic alteration in thyroid cancer. Unlike its high treatment response to selective BRAF inhibitor (PLX4032) in metastatic melanoma, the treatment response in thyroid cancer is reported to be low. The purpose of this study is to investigate the innate resistance mechanism responsible for this low treatment response to BRAF inhibitor in order to maximize the effect of targeted therapy. We examined the expression of feedback regulation mechanisms and alterations in the upper signal transduction pathway in thyroid cancer cell lines harboring BRAF mutation. Also we investigated the effect of dual inhibition from combinatorial therapy. Two thyroid cancer cell lines, 8505C (anaplastic thyroid cancer) and BCPAP (papillary thyroid cancer) were selected and treated with PLX4032 and its drug sensitivity were examined and compared. Further investigation on the changes in signals responsible for the different treatment response to PLX4032 was carried out and the same experiment was performed on orthotopic xenograft mouse models. Unlike BCPAP cells, 8505C cells presented drug

resistance to PLX4032 treatment and this was mainly due to increased expression of c-Met. Effective inhibitions of c-Met, p-AKT, and p-ERK were achieved after dual treatment with BRAF inhibitor (PLX4032) and c-Met inhibitor (PHA665752). Similar results were confirmed by *in vivo* study with orthotopic xenograft mouse model. c-Met-mediated reactivation of the PI3K/AKT pathway and MAPK pathway contributes to the relative insensitivity of BRAF (V600E) mutant ATC cells to PLX4032. Dual inhibition of BRAF and c-Met leads to sustained treatment response.



Key words : thyroid cancer, drug therapy, molecular targeted therapy, drug resistance, BRAF mutation

c-Met-mediated reactivation of PI3K/AKT signaling contributes to insensitivity of BRAF(V600E) mutant thyroid cancer to BRAF inhibition

Hyung Kwon Byeon

*Department of Medicine
The Graduate School, Yonsei University*

(Directed by Professor Eun Chang Choi)

I. INTRODUCTION

Thyroid cancer is the most commonly presenting malignant tumor of the endocrine system and it is reported that its incidence in women are three times higher than in men. Recently, the incidence of thyroid cancer is rapidly increasing over the world, and in our country the increase rate is so high that thyroid cancer ranked top in cancer incidence rates in women according to the annual report of cancer statistics in Korea, 2011.¹ Histologically, carcinoma comprises approximately 98% of all thyroid malignancies. In thyroid carcinomas, the papillary carcinoma originating from the follicular cells is the most commonly encountered isotype, which accounts for over 80% of all thyroid cancers, followed by the follicular carcinoma (10-15%) and anaplastic carcinoma (2-5%). Medullary carcinoma originating from the parafollicular C-cells makes up about 5-10% of all thyroid cancers.²⁻⁵ Surgery, postoperative

radioactive iodine therapy and Thyroid-stimulating hormone (TSH) suppression by L-thyroxine administration form the basis of the treatment of well differentiated thyroid cancers. Although these treatment options are successful in the majority of the patients, the results can be disappointing in some advanced stage cancers, despite aggressive managements including conventional chemotherapy and radiotherapy. Anaplastic carcinoma in particular, has a very poor prognosis since the average survival period from initial diagnosis is only five months despite aggressive multimodality treatment. This is because it exhibits a highly invasive character and shows extensive locoregional invasion or systemic progression to lung, bone, or liver at the time of initial diagnosis.⁶

Multiple genetic alterations or mutations are involved in the tumorigenesis of thyroid cancer.⁷ Thyroid somatic mutations include the mitogen-activated protein kinase (MAPK) signal transduction pathway. RET tyrosine kinase of the cell membrane from mutated genes activates the MAPK pathway and up-regulates intracellular transducers RAS and B type RAF (BRAF), which in turn activates mitogen-activated protein/extracellular signal-regulated kinase (MEK) and extracellular single-regulated kinase (ERK), thereby resulting in intranuclear signal transduction for various intracellular mechanisms including cellular proliferation, differentiation and survival. The most heavily studied and commonly found genetic alteration in thyroid cancer is the BRAF mutation. BRAF is a serine-threonine kinase which is activated and bound by RAS and

then translocated to the cell membrane. The most commonly identified BRAF mutation in thyroid cancer is the substitution of valine to glutamic acid at residue 600 (V600E) caused by the point mutation of nucleotide position 1799. BRAF (V600E) mutation is most common in papillary carcinomas however, it is found in a third of undifferentiated or anaplastic carcinomas. BRAF mutation causes constitutive BRAF kinase activity and sustained activation of MAPK cascade through phosphorylation of MEK and ERK kinase. BRAF mutation is closely related to aggressive clinical and pathologic features of thyroid cancer such as lymphatic metastases, extrathyroidal capsular invasion, advanced clinical stage, tumor recurrence, re-operation and cancer-related deaths. Particularly in cases of recurred BRAF mutant thyroid cancers or those with accompanying undifferentiated characteristics, it is common to show clinical resistance to radioactive iodine therapy due to decreased radioiodine avidity from functional alterations of the sodium iodide symporter.

Besides thyroid cancer, BRAF (V600E) mutation is also detected in approximately 50% of malignant melanoma, 15% of colorectal cancer and nearly all cases of hairy-cell leukemia.⁸⁻¹⁰ PLX4032 (Vemurafenib), a selective BRAF inhibitor has been recently approved by the FDA for the treatment of BRAF (V600E) mutant metastatic melanoma, which has been reported to improve progression-free survival and overall survival in 80% of patients and improved treatment response was also noted in hairy-cell leukemia.^{11,12} Despite the high treatment response of BRAF inhibitors such as PLX4032 in BRAF

mutant malignant melanoma, its effects are insignificant in other solid tumors harboring BRAF mutation. The therapeutic effect of PLX4032 in patients with BRAF mutant colorectal cancer is merely 5%, and the effect of Selumetinib, a MEK inhibitor, in thyroid cancer has no effect, contrary to expectations.^{13,14} This discrepancy in treatment response comes from the manifestation of innate resistance mechanisms against targeted therapeutic agents. For instance, selective BRAF inhibition in BRAF mutant colorectal cancer induces transient ERK signal suppression, but the levels are soon reaccumulated. This rebound phenomenon results from the reactivation of the MAPK pathway by signal elevation of HER1 (EGFR). Oncogenic BRAF induces CDC25C and suppression of HER1 (EGFR) expression however after treatment of PLX4032, CDC25C expression is suppressed from BRAF inhibition which in turn leads to increased expression of HER1 (EGFR).¹⁵ Whatsmore expression levels of various receptor tyrosine kinases (RTK) such as EGFR, HER2, Met, insulin-like growth factor 1 receptor (IGF1R) are increased in BRAF mutant colorectal cancer.¹⁶⁻¹⁷ On the basis of these findings, dual inhibition of BRAF and EGFR in BRAF mutant colorectal cancer resulted in continuous signal suppression of MAPK, thereby improving therapeutic efficacy by overcoming innate resistance mechanism.¹⁷

Regarding the fact that thyroid cancer also shows therapeutic resistance to BRAF inhibition as in colorectal cancer, the aim of the present study is to elucidate the innate resistance mechanism which has not been extensively

investigated to date in order to maximize the effect of targeted therapy. We examined the expression of feedback regulation mechanisms and alterations in the upper signal transduction pathway in various thyroid cancer cell lines harboring BRAF mutation. Also we investigated the effect of dual inhibition from combinatorial therapy.

II. MATERIALS AND METHODS

1. Cell culture

BRAF (V600E) mutant thyroid cancer cell lines, 8505C (anaplastic thyroid cancer) and BCPAP (papillary thyroid cancer) were maintained in 10% RPMI medium at 37°C with 5% CO₂ under humidified conditions.

2. Confirmation of c-Met expression and c-Met inhibitor-induced suppression of c-Met expression by Western blot analysis

Thyroid cell lines were washed with phosphate buffered saline (PBS) and were treated with lysis buffer (10 mM Tris-HCl (pH 7.4), 100 mM NaCl, 1mM EDTA, 1mM EGTA, 1mM NaF, 20mM Na₄P₂O₇, 2mM Na₃VO₄, 1% Triton X-100, 10% glycerol, 0.1% SDS, 0.5% deoxycholate) (Invitrogen, Camarillo, CA, USA), 1 mM phenylmethylsulfonyl fluoride (PMSF) and protease inhibitors cocktail (Sigma-Aldrich, St. Louis, MO, USA) and then harvested. The protein was centrifuged under 13,200 rpm for 10 minutes and the

supernatant was used for Western blot analysis where the protein amount was quantified with Pierce BCA Protein Assay Kit (Thermo, Rockford, IL, USA). The lysates were subjected to 10% sodium dodecyl sulfate (SDS)-polyacrylamide gel electrophoresis (PAGE) to separate proteins. An equal amount of protein (30 μ g) was loaded per well and the proteins were transferred onto p-c-Met (1:1000), p-AKT (1:1000), p-ERK(1:1000), GAPDH (1:1000) to be left at 4°C overnight incubation. The next day, it was thoroughly washed with Tris buffered saline (TBS) containing 0.1% Tween-20, and then reacted with secondary rabbit antibody (Jackson, West Grove, PA, USA) and anti-mouse antibody (Jackson) to be visualized on X-ray film using SuperSignal West Pico Chemiluminescent Substrate (Thermo).

3. Cell proliferation assay

Thyroid cells (8505C, BCPAP) were seeded in 96-cell well plates at a density of 1×10^3 cells per well and were incubated for 24 hours at 37°C with 5% CO₂. For each sample, it was treated with BRAF inhibitor of varying concentrations and was incubated for 24 and 48 hours. 2 mg/ml of 3-(4,5-dimethylthiazol-2-yl)-2,5-diphenyl-tetrazolium bromide (MTT) test solution (Sigma-Aldrich) were added to each well and after 4 hours of incubation, 100 μ g dimethyl sulfoxide (DMSO) was added for each well and optical density (OD) was measured at 570 nm.

4. Immunohistochemical analysis

The tumor tissue samples from mice were processed for paraffin section and consequently were undergone deparaffinization with xylene and ethanol. Antigen retrieval was done for 15 minutes followed by reaction with H₂O₂ for 10 minutes and blocking (10% normal goat serum + 0.01% bovine serum albumin (BSA) + dilution) for 1 hour. The slides were then incubated overnight at 4°C with primary anti-c-Met and AKT antibody (1:200). Next, the slides were treated with secondary anti-rabbit antibodies (1:500) for 1 hour and reacted using DAB histochemistry kit (Life technologies, Rockford, IL, USA). Finally the slides were stained with hematoxylin and processed with mounting solution (DAKO) and visualized using a microscope.

5. FACScan with Annexin V-fluorescein isothiocyanate (FITC) / propidium iodide (PI) staining

3×10^5 cells were seeded onto 6-well culture dishes and cultured and after 24 hours of starvation, the cells were treated with 1 μM PLX4032 and cultured with time variation. Culture fluid was removed and the cells were washed three times with PBS, transferred in 1.5 ml tubes, and resuspended in Annexin V-FITC Apoptosis Detection kit I (Bio-vision, San Francisco, CA, USA) binding buffer and Annexin V-FITC. After 5 minutes reaction at room temperature, apoptosis was detected using BD FACSVerser (Flow cytometer).

6. Orthotopic xenograft mouse model

8505C cells were harvested and 1×10^5 cells suspended in 5 μ l PBS were injected orthotopically in the right thyroid gland of male athymic nude BALB/c mice, aged 6 weeks (Orientbio Inc., Seongnam-si, Korea) using a 25 μ l Hamilton syringe (Hamilton Company, Reno, NV, USA). After tumor cell implantation, the mice were randomized into 4 groups. The control group was treated with DMSO and the other 3 groups were each injected with PLX4032, PHA665752, PLX4032 and PHA665752 combination respectively, for 3 weeks 9 times. The animals were then euthanized and Western blot analysis, H&E staining, and immunohistochemical analysis were carried out from tissue samples. All procedures of the animal experiment were approved by the Committee for ethics in animal experiments of Yonsei University College of Medicine and all animals in the experiment were handled in accordance with the Guide for the care and use of laboratory animals in Department of laboratory animal resources, Yonsei University College of Medicine.

7. Terminal deoxynucleotidyltransferase-mediated dUTP-biotin nick end labeling (TUNEL) assay

Cells were fixed in 1% paraformaldehyde (PFA) containing PBS (pH 7.4) at room temperature for 10 minutes, and after washing, the cells were incubated with 5 μ l TUNEL enzyme (Roche Molecular Biochemicals, Basel, Switzerland) and 45 μ l TUNEL label (Roche Molecular Biochemicals) mixture for 1 hour at

37°C. The stained cells were then visualized with confocal microscopy (Carl Zeiss, Oberkochen, Germany) at 515~565 nm.

8. Immunofluorescence

1x10⁵ cells per well were seeded onto 6-well culture dishes and were incubated for 24 hours at 37°C with 5% CO₂. After PLX4032 treatment and media suction, the cells were fixed in PFA for 20 minutes at room temperature and after 5 minutes treatment of 1 % Triton, blocking (PBS+ 1% BSA+ 10% normal goat serum) was done for 1 hour. The slides were then treated with primary antibody (1:200) and were incubated overnight at 4°C. After 3 hours reaction with secondary antibody (1:500), the slides were visualized with confocal microscopy (Carl Zeiss) at 450 nm.

9. Pathscan RTK signaling antibody array

An antibody array for simultaneous detection of RTK and key signaling nodes was used (Cell signaling technology Inc., Danvers, MA, USA). All target RTKs or kinases were detected with a phospho-specific or a pan-tyrosine recognizing antibody as indicated in the manual of the array. 8505C cells were treated with DMSO or PLX4032 for 9 hours. The cells were then harvested and cell lysates were prepared according to the manufacturer's instructions and hybridized to the slides containing pre-spotted target-specific antibodies. Detection was done using a biotin-streptavidin-conjugated antibody with an image analysis software.

Relative levels of phosphorylated RTK or other signaling proteins in DMSO-treated cells compared to PLX4032-treated cells were calculated from three independent experiments.

10. Hepatocyte growth factor (HGF) ELISA

The media was gathered and concentrated before Western blot analysis. Quantikine ELISA human HGF (R&D Systems co., Minneapolis, MN, USA) was used on concentrated media. 150 μ l Assay diluent RD1W was applied to 50 μ l media and incubated for 2 hours. Then it was washed 4 times with 400 μ l wash buffer solution and was incubated for 1.75 hours after treatment of 200 μ l HGF conjugate. It was then washed 4 times again with the wash buffer and after dimming the light, 50 μ l substrate solution was added and incubated for 30 minutes, followed by treatment of 50 μ l stop solution for measurement of OD at 450 nm.

11. Transient transfection of c-Met and RNA interference (siRNA)

2×10^5 cells per well were seeded onto 6-well culture dishes containing 2ml antibiotic-free medium supplemented with 10% fetal bovine serum (FBS). The cells were incubated at 37°C with 5% CO₂ until the cell monolayers achieved 60-80% confluence. Next, 500 μ l optimum and 10 μ l RNAiMAX, and 500 μ l optimum and 5 μ l RNAi were mixed and left at room temperature for 5 minutes, and then mixed together. After 20 minutes, droplets of the mixture were applied

at the cells and left to react for 6 hours. Thereafter, the medium was changed to 10% FBS and penicillin-streptomycin supplemented medium and the cells were incubated at 37°C with 5% CO₂ for 48 hours. Subsequently PLX4032 was treated for 6 hours and the cells were harvested and confirmed by Western blot analysis.

12. Statistical analysis

All the data were derived from three independent experiments, and the parameters were expressed as the means ± SD. “Student’s” t test and one way ANOVA were performed using SPSS 20.0 statistical software (SPSS, Chicago, IL, USA). A $P < 0.05$ was considered statistically significant (* $P < 0.05$; ** $P < 0.01$; *** $P < 0.001$).

III. RESULTS

1. PLX4032 shows different drug sensitivity against different BRAF (V600E) mutant thyroid cancer cell lines

To evaluate the drug sensitivity of BRAF inhibitor, PLX4032 on BRAF mutant thyroid cancer, the drug effect was investigated using two different types of thyroid cancer cell lines harboring BRAF (V600E) mutation, 8505C (anaplastic thyroid cancer) and BCPAP (papillary thyroid cancer). Cell lines were treated with PLX4032 for 24 hours and cell viability was analyzed by MTT assay. The

results revealed that 8505C cells showed some degree of proliferation despite drug treatment, however BCPAP cells presented approximately 40% apoptosis.

(Fig. 1)

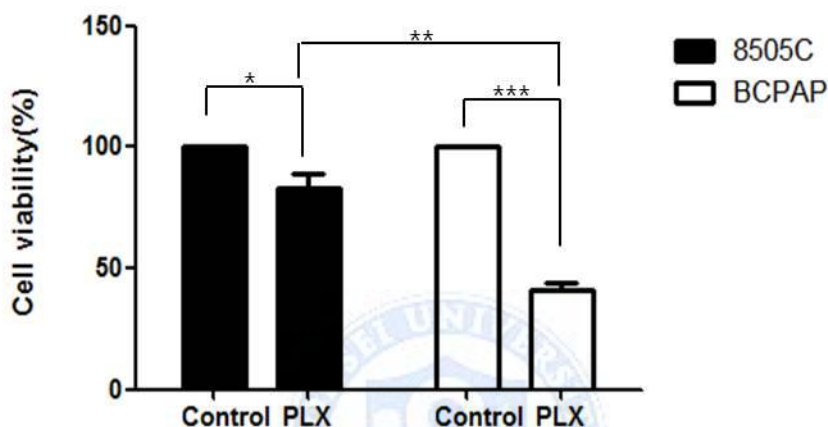


Fig. 1. Differential drug sensitivity of BRAF (V600E) mutant thyroid cancer cell lines 8505C and BCPAP to PLX4032 treatment. MTT assay done after treatment with 3 μ M PLX4032 for 24 hours showed that the cell viability was higher for the 8505C. (*: $p < 0.05$, **: $p < 0.01$, ***: $p < 0.001$)

To determine whether the PLX4032-induced cell death was due to apoptosis, several assays detecting the level of apoptosis were performed. The Western blot analysis from the treatment of PLX4032 of various time periods showed constant and unaffected survival of 8505C cells, unlike BCPAP cells. (Fig. 2) From the FACS using Annexin V-FITC / PI staining, PLX4032-induced cell

apoptosis was less prominent in 8505C cells as compared to BCPAP cells. (Fig. 3) Similar results were noted from TUNEL assay which could assess apoptosis. (Fig. 4)

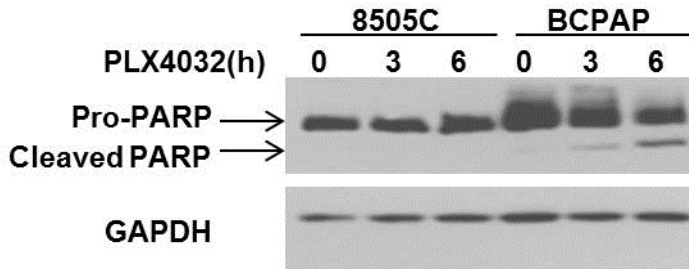


Fig. 2. Western blot analysis after treatment with 1 μ M PLX4032 of increasing treatment times. PLX4032-induced cleaved PARP expression was more prominent in the BCPAP cells as compared to the 8505C cells.

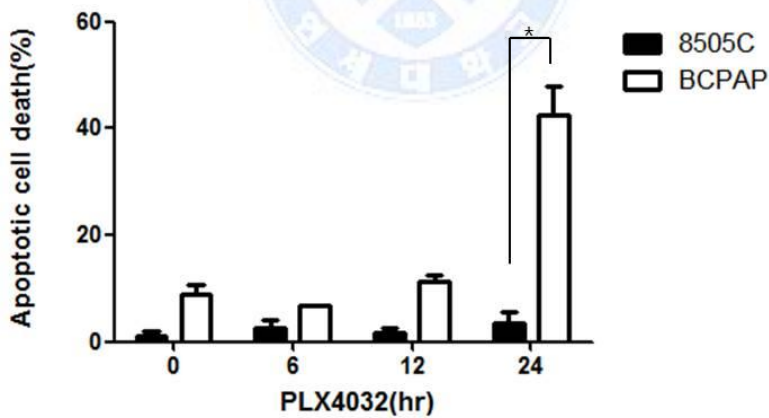


Fig. 3. Analysis of apoptotic cell death with Annexin V-FITC/PI staining. 1 μ M PLX4032 was treated for 6, 12, and 24 hours to both 8505C and BCPAP cells. Apoptosis was substantially increased in the BCPAP cells. (*: $p < 0.05$)

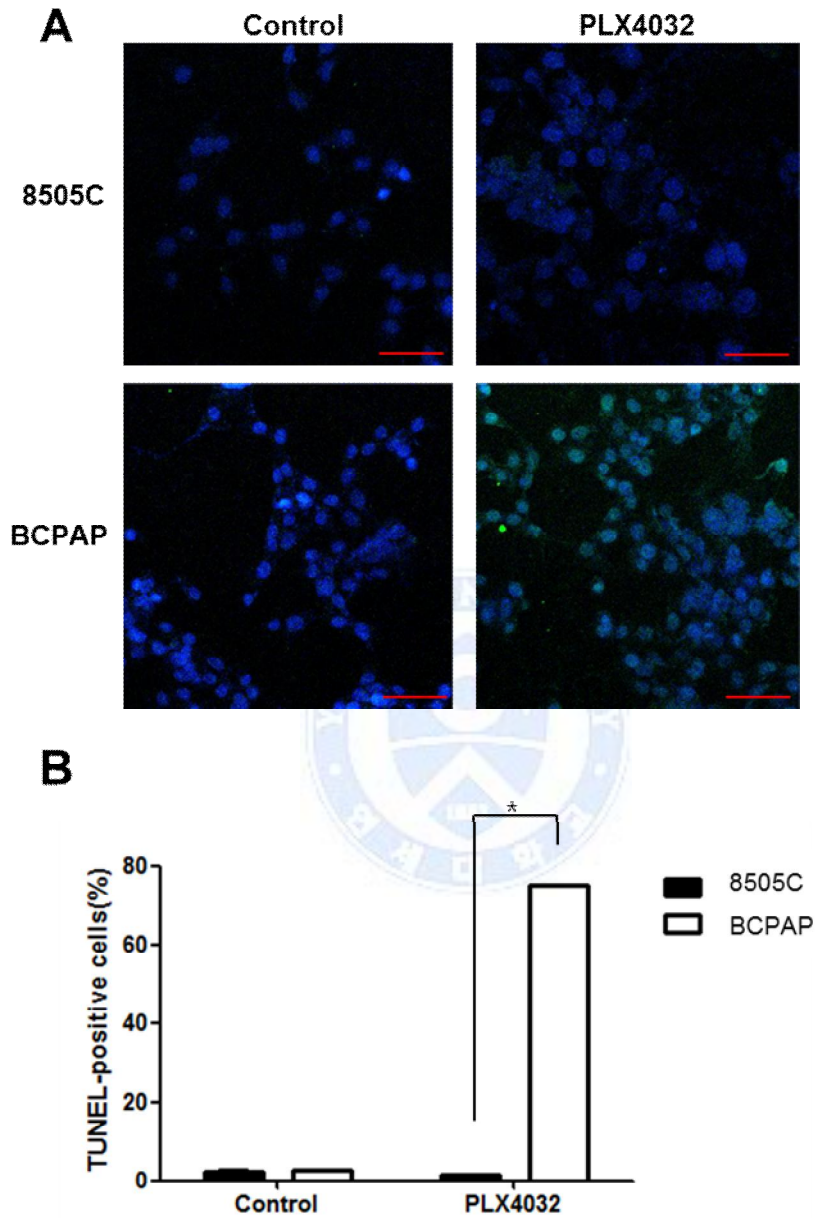


Fig. 4. TUNEL assay. (A) Cells were treated with 1 μ M PLX4032 for 6 hours. PLX4032-induced TUNEL-positive cells were more prominently increased in BCPAP cells compared to 8505C cells. (B) Quantification of apoptotic cells

from TUNEL assay. TUNEL-positive cells were significantly increased in BCPAP cells after PLX4032 treatment. (*: $p < 0.05$)

2. PLX4032 induces over-expression of p-c-Met and subsequently over-expression of PI3K / AKT pathway in BRAF (V600E) mutant anaplastic thyroid cancer cell (8505C)

When 8505C cells were treated with PLX4032 and cell viability assessed until 2 days, it was unaffected, moreover increased with respect to control, by the drug treatment. (Fig. 5) According to RTK array after PLX4032 treatment, specific over-expression of c-Met was confirmed. (Fig. 6)

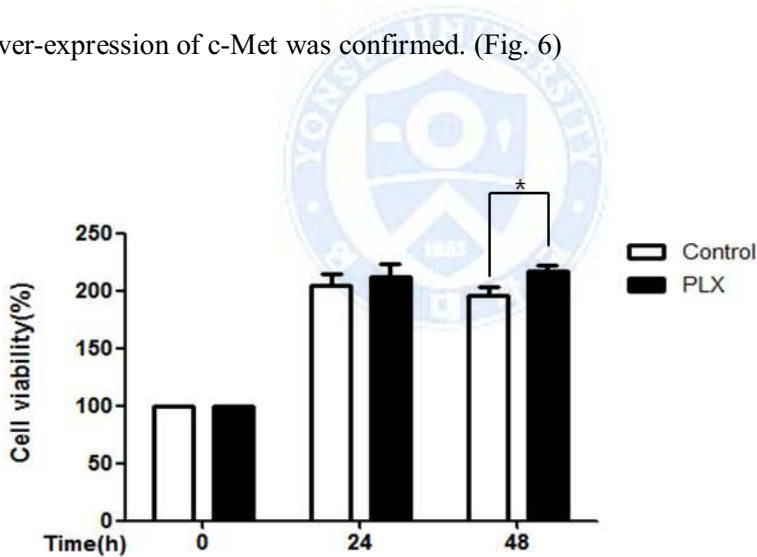


Fig. 5. MTT assay done after treatment with 3 μ M PLX4032 until 48 hours in 8505C cells. Cell proliferation was unaffected by the PLX4032 treatment. (*: $p < 0.05$)

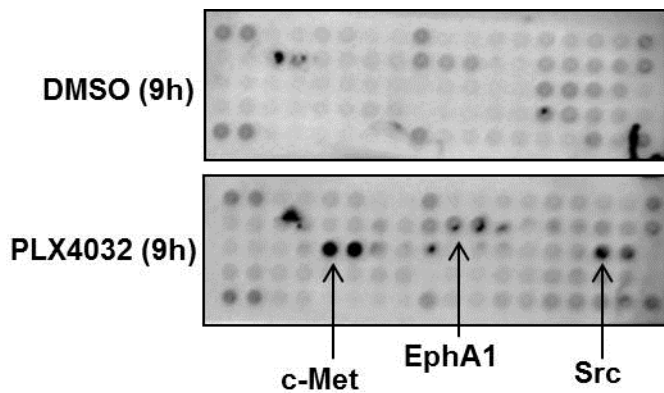


Fig. 6. RTK array after treatment with 3 μ M PLX4032 for 9 hours in 8505C cells. c-Met expression was specifically detected.

Analysis of p-c-Met expression in the 8505C and BCPAP cells by Western blot analysis revealed that p-c-Met expression was significantly increased in 8505C cells according to increased treatment times of PLX4032 whereas it was unchanged in BCPAP cells. (Fig. 7)

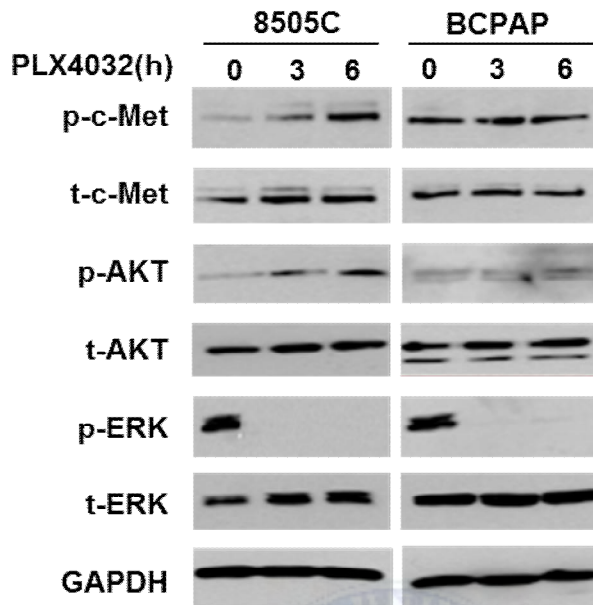


Fig. 7. Western blot analysis after treatment of 1 μ M PLX4032 for 3 and 6 hours in both 8505C and BCPAP cells. Unlike BCPAP cells, p-c-Met expression was increased through increased treatment times of PLX4032 in 8505C cells.

To investigate the PLX4032-induced over-expression of p-c-Met, the BRAF inhibitor was treated to 8505C cells at different levels of concentrations and treatment times and expression levels of p-c-Met were assessed by Western blot analysis. Expressions of p-c-Met were constantly increased according to treatment of increased concentrations of PLX4032 and subsequently p-AKT expressions were also increased. (Fig. 8) Similar patterns were noted also according to increased drug treatment times where p-c-Met sequentially increased until 9 hours. (Fig. 9)

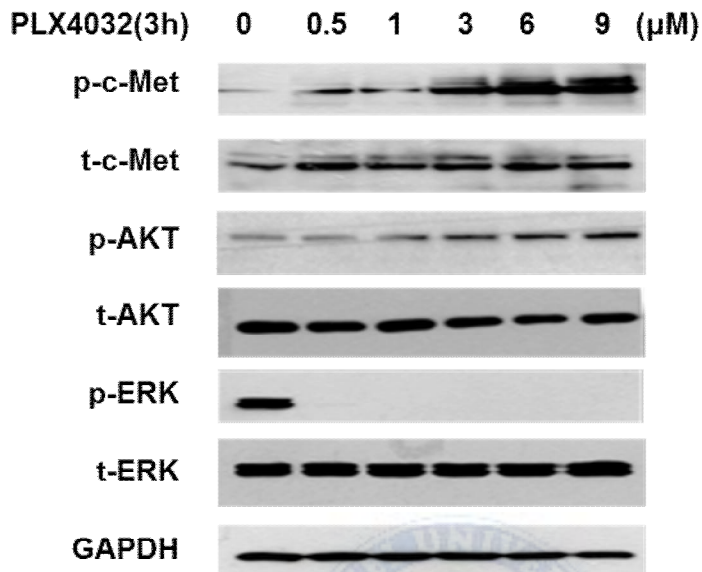


Fig. 8. Western blot analysis after treatment of PLX4032 of increasing dosages for 3 hours in 8505C cells. p-c-Met expression levels were increased and p-AKT levels were subsequently increased according to increased dosages of PLX4032 treatment.

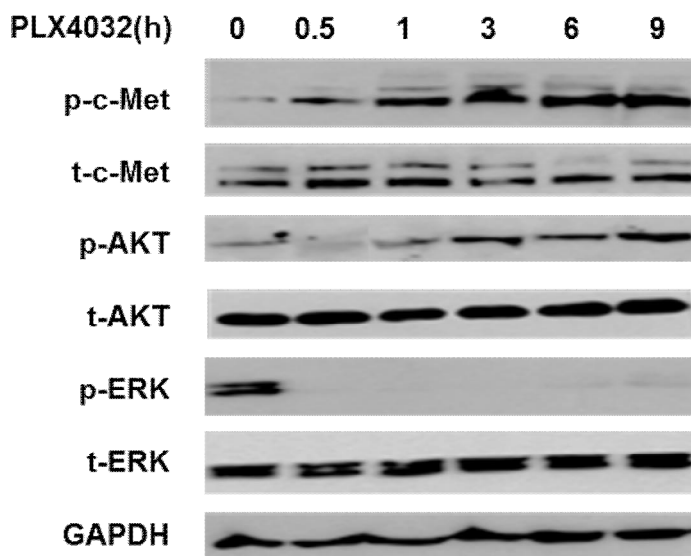


Fig. 9. Western blot analysis after treatment of 1 μ M PLX4032 of increasing treatment times in 8505C cells. p-c-Met expression levels were increased and p-AKT levels were subsequently increased according to increased treatment times of PLX4032.

The therapeutic effect of PLX4032 in 8505C cells could be verified by the decreased expression of p-ERK. However p-ERK levels showed mild rebound increase after 9 hours treatment of PLX4032 (data not shown). Expression levels of p-AKT were increased following the increased expression of p-c-Met. When c-Met was knocked down and PLX4032 treated with increasing times, both c-Met and p-AKT expression levels were decreased. (Fig. 10)

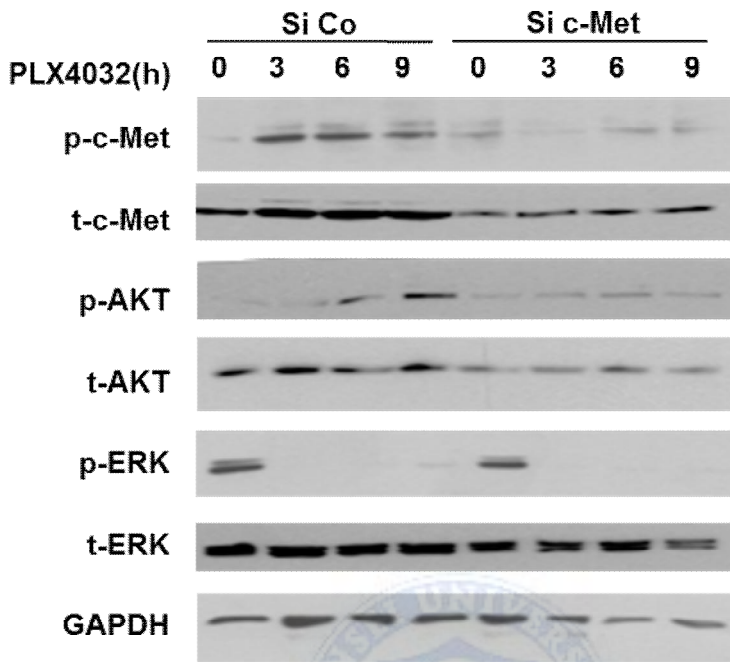


Fig. 10. 8505C cells transfected with c-Met small interfering RNA (siRNA) or negative control siRNA were treated with 1 μ M PLX4032 for 3,6, and 9 hours. Following knockdown of c-Met, p-c-Met and p-AKT expression levels were constantly decreased.

3. Inhibition of c-Met can reverse the over-expression of PI3K / AKT pathway after treatment of PLX4032 in BRAF (V600E) mutant anaplastic thyroid cancer cell (8505C)

Following the combinatorial treatment of PLX4032 with PHA665752, a c-Met inhibitor in 8505C cells, p-c-Met levels were not increased and p-AKT expression was considerably decreased. (Fig. 11) Following single treatment of

PHA665752, p-c-Met expression levels were decreased however p-AKT and p-ERK levels were unchanged. (Fig. 12)

From the MTT and TUNEL assay, drug-induced cell apoptosis was more prominent following combinatorial treatment of PLX4032 and PHA665752 than single agent treatment, and same results were noted from Western blot analysis of PARP expression. (Fig. 13-15)

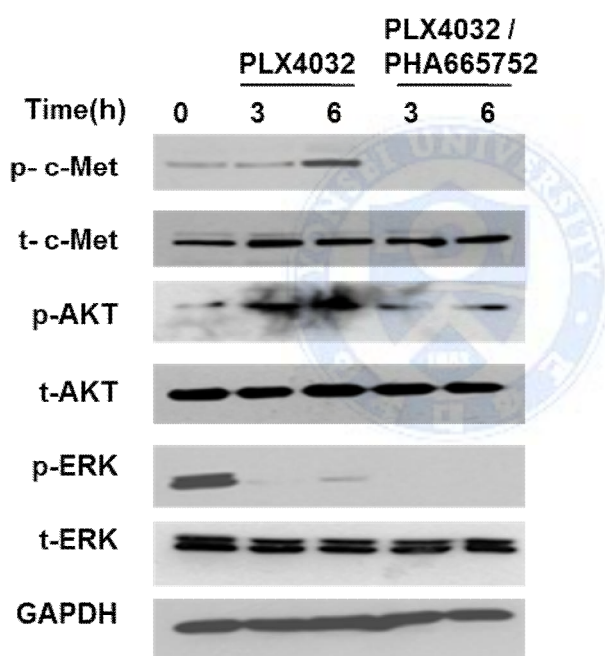


Fig. 11. Western blot analysis of each after treatment of 1 μ M PLX4032 and dual treatment of 1 μ M PLX4032 and 0.5 μ M PHA665752 for 3 and 6 hours in 8505C cells. The increased levels of p-c-Met and p-AKT expression after PLX4032 treatment were suppressed together with p-ERK suppression by combinatorial treatment of PLX4032 and PHA665752.

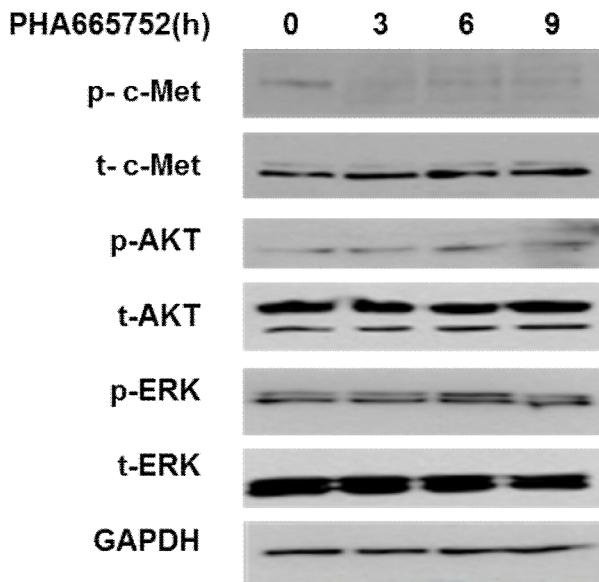


Fig. 12. Western blot analysis after treatment of 0.5 μ M PHA665752 for 3,6, and 9 hours in 8505C cells. p-c-Met expression levels were decreased however p-AKT and p-ERK levels were unaffected.

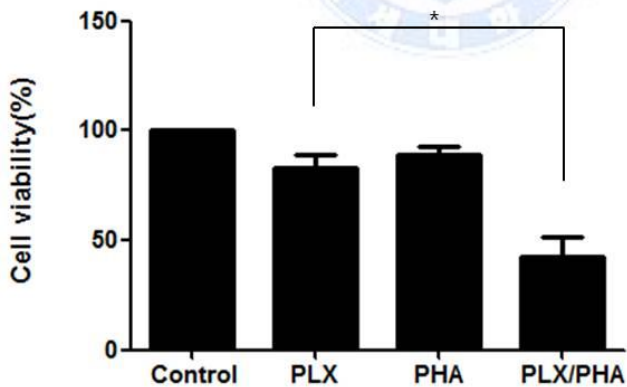


Fig. 13. MTT assay done after different drug treatment conditions for 24 hours in 8505C cells. Cell proliferation was significantly decreased after dual treatment of 1 μ M PLX4032 and 0.5 μ M PHA665752. (*: $p < 0.05$)

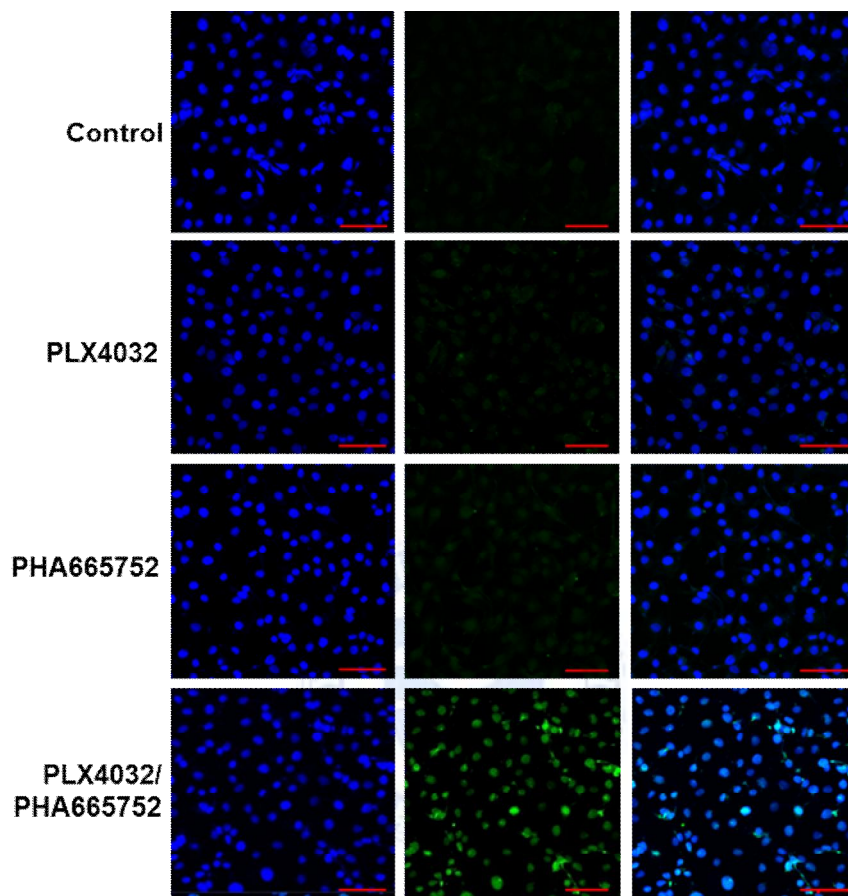


Fig. 14. TUNEL assay. 8505C cells were each treated under different drug regimens. TUNEL-positive cells were most prominently increased after combinatorial treatment of 1 μ M PLX4032 and 0.5 μ M PHA665752 for 6 hours.

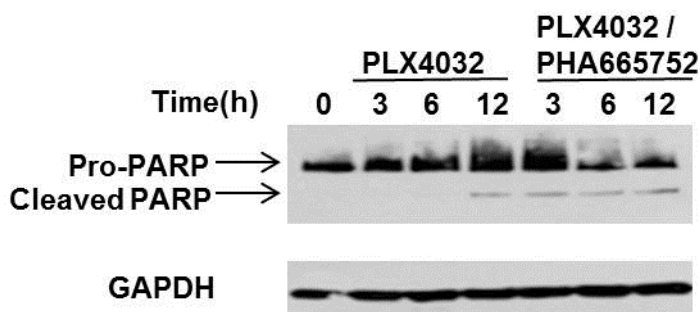


Fig. 15. Western blot analysis of each after treatment of 1 μ M PLX4032 and dual treatment of 1 μ M PLX4032 and 0.5 μ M PHA665752 in 8505C cells. Drug-induced cleaved PARP expression was more prominent following combinatorial treatment of PLX4032 and PHA665752.

4. PLX4032 induces the expression of HGF in BRAF (V600E) mutant anaplastic thyroid cancer cell (8505C)

HGF ELISA was done in 8505C cells showing over-expression of c-Met and BCPAP cells with unchanged levels of c-Met following treatment of PLX4032. The results demonstrated that levels of HGF, the c-Met ligand were considerably increased in 8505C cells but unchanged in BCPAP cells. (Fig. 16) The increased HGF expression levels from PLX4032 treatment were mainly noted in the media containing 8505C cells by Western blot analysis. (Fig. 17) Western blot analysis was done after treatment of PLX4032, PHA665752, and HGF. (Fig. 18) Expression of p-c-Met was increased following PLX4032 treatment, more increased after HGF treatment, and most increased following treatment of both. Similar results were also noted for p-AKT. After dual

treatment of PLX4032 and PHA665752, expression levels of p-c-Met, p-AKT, and p-ERK were all decreased.

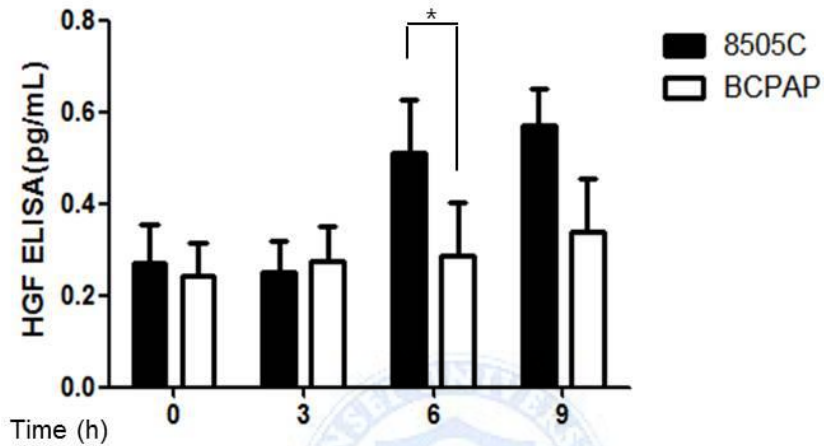


Fig. 16. HGF ELISA after 1 μ M PLX4032 treatment of increasing duration in 8505C and BCPAP cells. HGF levels were significantly increased in 8505C cells. (*: p<0.05)

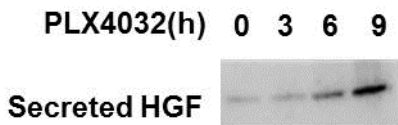


Fig. 17. Western blot analysis after treatment of 1 μ M PLX4032 for 3,6, and 9 hours in 8505C cells. HGF expression levels within the media (secreted HGF) were increased.

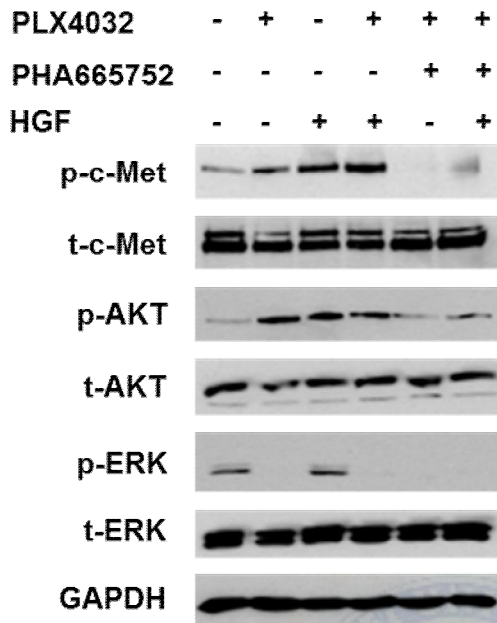


Fig. 18. Western blot analysis after different treatment conditions consisting of 1 μ M PLX4032, 0.5 μ M PHA665752, and 30ng/ml HGF for 9 hours in 8505C cells. p-c-Met expression was increased together with p-AKT expression after PLX4032 and HGF treatment but were effectively suppressed after combinatorial treatment of PLX4032 and PHA665752.

5. Combinatorial treatment of PLX4032 and PHA665752 can inhibit the tumor growth in an orthotopic xenograft mouse model

To determine whether the above-mentioned results and treatment patterns were consistent *in vivo*, an orthotopic xenograft mouse model was established by injecting 8505C cells in thyroid glands of nude BALB/c mice. Tumor formation was confirmed at 3 weeks post-injection, and the mice were randomly divided

into four groups of four. For each groups, DMSO, PLX4032, PHA665752, PLX4032 and PHA665752 combination were treated respectively, 3 times a week for 3 weeks. The tumor size was similar or slightly larger in the PLX4032 and PHA665752 single treatment group with reference to the control group, however the tumor size was significantly smaller in the combinatorial treatment group. (Fig. 19)

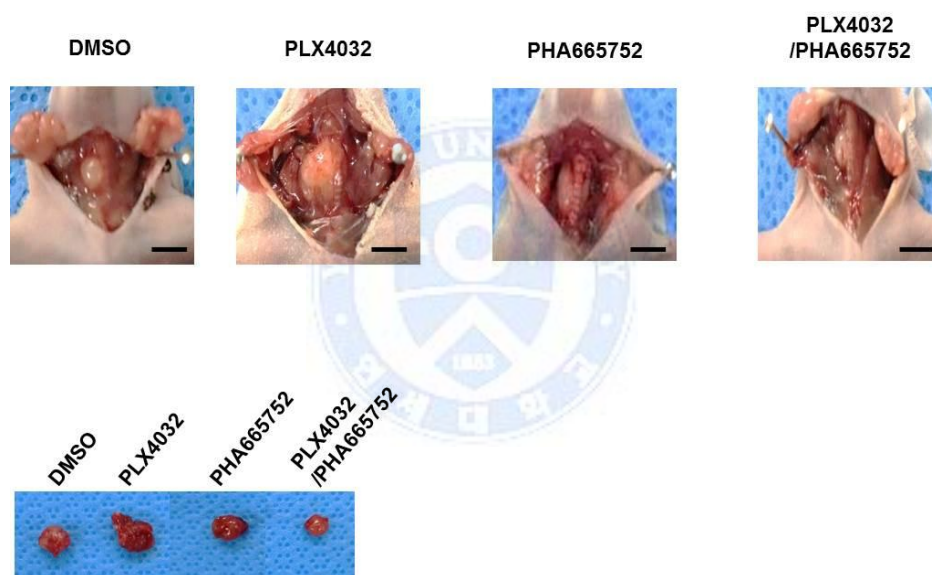


Fig. 19. Treatment response to PLX4032 and PHA665752 in a xenograft mouse model orthotopically injected with 8505C cells. The 8505C cells injected mice were randomly divided into four groups with different treatment conditions as follows: DMSO (20mg/kg/day), PLX4032 (20mg/kg/day), PHA665752 (10mg/kg/day), and combinatorial PLX4032 (20mg/kg/day) and PHA665752 (10mg/kg/day) treatment. The tumor size was slightly larger or similar in the

single agent treatment group when compared to control group, however it was significantly smaller in the combinatorial treatment group.

From the assessment of tumor volume and weight, the values were larger in the mice of PLX4032 single treatment group compared to the DMSO treated mice, however both values were significantly lower in the mice with combinatorial treatment of PLX4032 and PHA665752. (Fig. 20) From the analysis of protein expression levels in tumor specimens, p-c-Met expression was increased in PLX4032 single treatment group however it was considerably decreased in combinatorial drug treatment group. (Fig. 21) Levels of p-AKT expression were also high in PLX4032 single treatment group and significantly low in combinatorial treatment group.

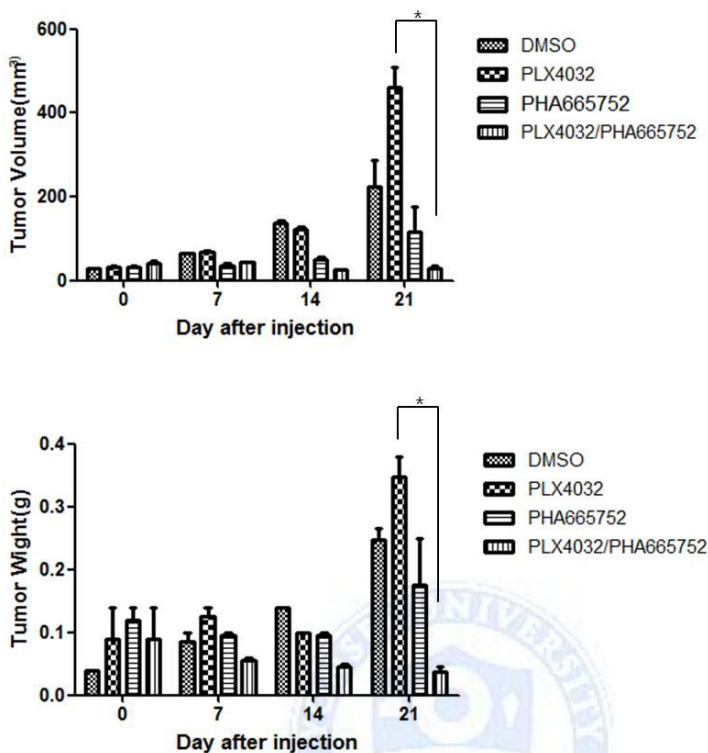


Fig. 20. Assessment of tumor volume and weight 3 weeks following different drug treatments in orthotopic xenograft mouse model. 8505C cells were orthotopically injected in thyroid glands of BALB/c nude mice and randomly divided into four groups with different treatment conditions as follows: DMSO (20mg/kg/day), PLX4032 (20mg/kg/day), PHA665752 (10mg/kg/day), and combinatorial PLX4032 (20mg/kg/day) and PHA665752 (10mg/kg/day) treatment. Both tumor size and volume were larger in PLX4032 single agent treatment group when compared to control group, however the values were significantly smaller in the combinatorial treatment group. (*: $p < 0.05$)

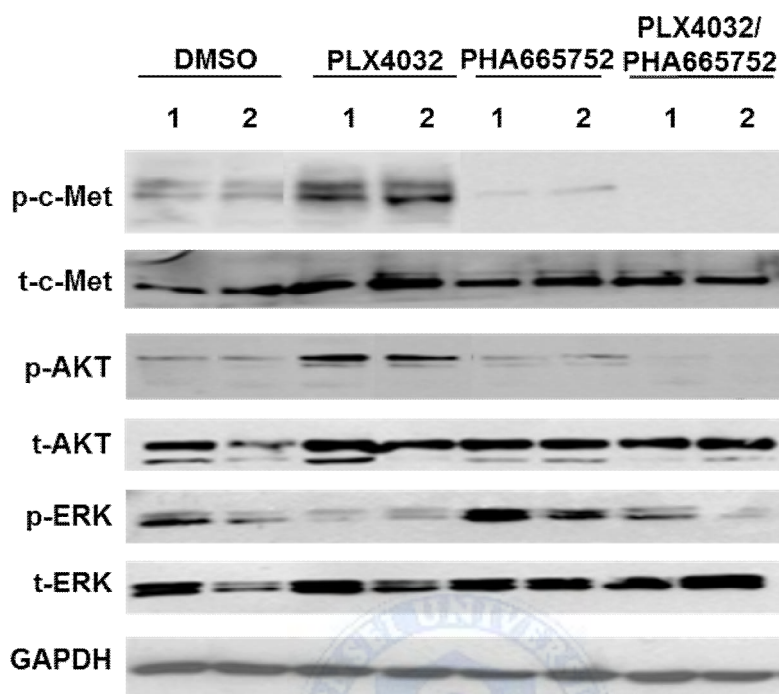


Fig. 21. Western blot analysis of intratumoral protein expression after drug treatment in tumor specimens of 8505C cells orthotopically-injected mice. Both p-c-Met and p-AKT expression levels were increased in PLX4032 single treatment group however they were considerably decreased in combinatorial drug treatment group.

Histopathological analysis was performed by hematoxylin and eosin (H & E) staining from tumor specimens of mice from each treatment group. (Fig. 22) The tumors from drug-treatment groups generally presented tumor capsule formation with pushing margins whereas the tumor of the control group showed irregular infiltrative growth with no evidence of tumor capsule. More

specifically, the PLX4032 single treatment group showed further aggressive features such as frequent extracapsular extension, lymphovascular invasion, and perineural invasion. The combinatorial drug treatment group however presented no tumor capsule invasion with lymphocytes aggregating around the tumor and absence of lymphovascular invasion and perineural invasion. Cellular change of degeneration and decreased cell viability was noted in all drug-treatment groups when compared to highly viable tumor cells of the control group, but the degree was most prominent in the combinatorial treatment group. Furthermore, immunohistochemistry to demonstrate intratumoral protein expression levels in tumor tissues of each treatment groups confirmed high detection levels of p-c-Met and p-AKT in the PLX4032 single treatment group. Both levels were however markedly decreased with low detection of p-ERK in the combinatorial drug treatment group. (Fig. 23)

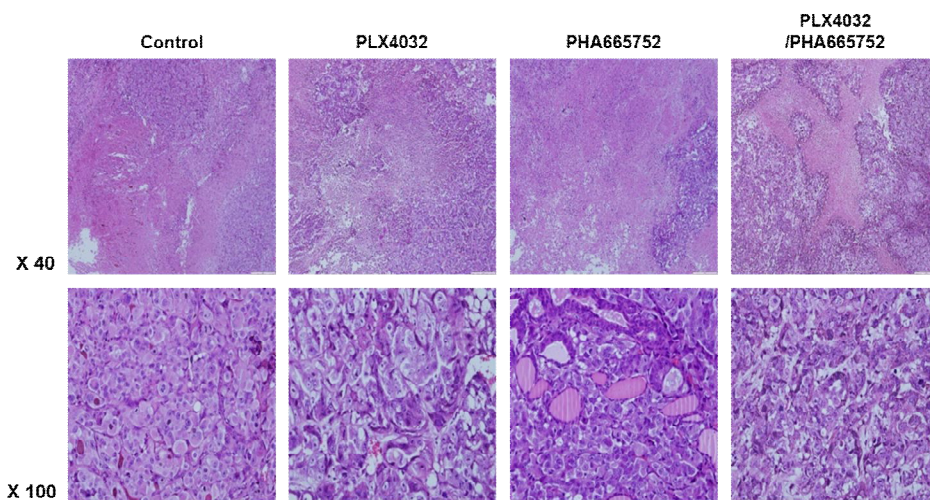


Fig. 22. Histopathological analysis confirmed by H & E staining from tumor tissue samples derived from mice of each group with different drug treatment conditions. (Control, PLX4032, PHA665752, PLX4032 and PHA665752) On x40 magnification, the tumors of drug-treatment group generally presented tumor capsule formation with pushing margins as supposed to irregular infiltrative tumor growth in the control group. Specifically, the PLX4032 single treatment group showed further aggressive features such as frequent extracapsular extension with presence of lymphovascular invasion and perineural invasion. The combinatorial drug treatment group however presented no tumor capsule invasion with lymphocytes aggregating around the tumor. Lymphovascular invasion and perineural invasion were not found. On x100 magnification, cellular degenerative change and degree of decreased cell viability was most prominent in the combinatorial treatment group.

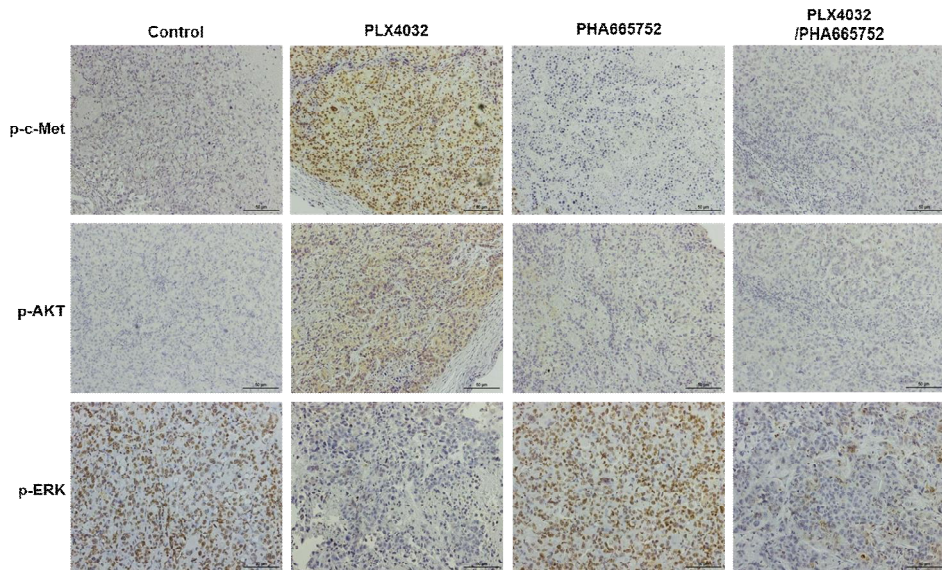


Fig. 23. Immunohistochemistry evaluation of tumor tissues from each treatment group. (Control, PLX4032, PHA665752, PLX4032 and PHA665752) Compared to the control group, p-c-Met and p-AKT detection levels were high in the PLX4032 single treatment group. In the combinatorial PLX4032 and PHA665752 treatment group, detection levels of p-c-Met, p-AKT, and p-ERK were all markedly low.

IV. DISCUSSION

Anaplastic thyroid cancer which comprises approximately 5% of all thyroid carcinomas is considered highly aggressive and presents an extremely poor prognosis since it is resistant to conventional treatment modalities. In addition, conventional chemotherapy and radiation frequently cause serious

post-treatment complications such as extensive tissue fibrosis, wound cicatrization, and edema and due to the adverse effects to the head and neck region such as difficulties in swallowing and voice change, it thereby leads to eventual deterioration of patients' quality of life. Therefore it is imperative for development of tumor-specific targeted agents with relatively low toxicity.

The RAF kinase is an important transducer in the RAS → MEK → MAP/ERK pathway which is involved in cellular growth, differentiation and carcinogenesis. The BRAF kinase is the most potent activator of this signal cascade and the gene is located at chromosome 7. Various point mutations of BRAF can occur in thyroid cancer but the most common mutation is the replacement of nucleotide position 1799 of exon 15, thymine to adenine, which results in the substitution of valine to glutamic acid at residue 600 of the protein (V600E).⁷ BRAF (V600E) mutation is present in 29-70% of papillary thyroid cancer,¹⁸⁻²¹ approximately 26% of anaplastic thyroid cancer,²² and other malignancies such as colorectal cancer, ovarian cancer, lung cancer, and hepatobiliary cancer.¹⁰ There have been numerous studies to investigate the role of BRAF genetic mutation in carcinogenesis and to develop effective targeted therapeutic agents on the basis of these results. PLX4032 (Vemurafenib), a typical selective BRAF inhibitor, have shown 80% treatment response in BRAF (V600E) mutant melanoma but was not as effective in other solid tumors harboring BRAF (V600E) mutations therefore there have been many studies on the mechanism of drug resistance. According to Corcoran et al., when PLX4032 was treated to

BRAF mutant colorectal cancer, p-ERK signal was transiently suppressed however it was soon re-activated due to EGFR-mediated RAS and CRAF activation.¹⁷ Over-expression of p-EGFR was also noted and therefore when both BRAF and EGFR signals were suppressed, the MAPK signal pathway could be effectively suppressed thereby improving the therapeutic efficacy. Furthermore, Nehs et al. reported that PLX4032 could suppress tumor cell growth in an orthotopic mouse model of BRAF mutant anaplastic thyroid cancer.²³ Montero-Conde et al. showed that when inhibitors of BRAF and MEK were treated in BRAF mutant melanoma, ERK signal was constantly suppressed, however in BRAF mutant thyroid cancer, only transient suppression was ERK signal was achieved, and this rebound phenomenon was the result of HER3 signal elevation.²⁴ That is, HER2 was coactivated with HER3 which in turn re-activated RAS-ERK signal pathway and this innate mechanism effects in the decreased response of tumor growth suppression by BRAF inhibition. In this process, neuregulin-1 (NRG1), a HER3 ligand, was induced by PLX4032, and this was also involved in the activation of HER3-mediated pathway. Therefore, in the present study, we investigated in detail the innate resistance mechanism against BRAF inhibitor in thyroid cancer which has not been extensively studied, to provide an effective targeted therapy.

In the present study, changes in the signaling pathway following PLX4032 treatment in two different thyroid cancer cell lines, 8505C and BCPAP, harboring BRAF (V600E) mutation were investigated. Interestingly, contrary

responses were discovered between 8505C and BCPAP, that is, resistance against PLX4032 was demonstrated in 8505C cells whereas increased apoptosis and consequently enhanced treatment response were shown in BCPAP cells. (Fig. 1-4) The causative mechanism for this different drug sensitivity in different types of BRAF (V600E) mutant thyroid cancer is unknown and is beyond the scope of this study but further investigation would be needed. On the basis of these findings, when 8505C cells were treated with selective BRAF inhibition, it could be inferred that an innate resistance mechanism was responsible for this decreased treatment response, and to further elucidate this resistance mechanism, alterations in signaling following PLX4032 treatment of varying drug concentrations and treatment times in 8505C cells were investigated. The results showed that expression levels of p-c-Met were specifically increased and p-AKT levels were consequently increased as well. (Fig. 6-9) These results suggest that BRAF inhibition in 8505C cells leads to over-expression of c-Met which in turn results in re-activation of MAPK pathway and also PI3K / AKT pathway. The rebound phenomenon of the p-ERK signal from PLX4032 treatment could be observed to a minimal degree as a late response in the present study. The BRAF inhibition-mediated c-Met over-expression mainly affects the PI3K / AKT pathway and further studies are warranted to elucidate the core mechanism of ERK signal reactivation from BRAF inhibition. Following the treatment of PLX4032, the expression of HGF, the only ligand of c-Met was induced and this result demonstrates that the

PLX4032-mediated over-expression of c-Met is caused by the induction of the c-Met ligand. (Fig. 16,17) On the basis of the findings that c-Met is increased from PLX4032 treatment in 8505C cells, combinatorial treatment of BRAF inhibitor (PLX4032) and c-Met inhibitor (PHA665752) resulted in effective suppression of both p-AKT and p-ERK, suggesting enhanced therapeutic efficacy. (Fig. 12-15) Furthermore, the results of the *in vitro* study was confirmed in *in vivo* animal experiments. (Fig. 19-23)

In summary, this study demonstrates that different treatment responses are shown in different types of thyroid cancer harboring BRAF (V600E) mutation from treatment of selective BRAF inhibitor. Particularly in 8505C cells which presented decreased responses of cellular growth inhibition and tumor suppression, there exists an innate resistance mechanism to BRAF inhibition, mediated by the increased expression of c-Met. Therefore, in BRAF (V600E) mutant anaplastic thyroid cancer which is resistant to PLX4032, the combinatorial treatment of BRAF inhibitor and c-Met inhibitor can overcome the limitation of single agent therapy and maximize the specific anti-tumor effect of targeted therapy. Whatsmore, its clinical implications are expected to be greatly extended, forming the basis of optimal personalized combinatorial targeted therapy.

V. CONCLUSION

c-Met-mediated reactivation of the PI3K/AKT pathway and MAPK pathway contributes to the relative insensitivity of BRAF (V600E) mutant ATC cells to PLX4032. Dual inhibition of BRAF and c-Met leads to sustained treatment response and this could form the basis of personalized optimal targeted therapy for thyroid cancer.



REFERENCES

1. The Korea Central Cancer Registry, National Cancer Center. Annual report of cancer statistics in Korea in 2011, Ministry of Health and Welfare, 2013.
2. National Cancer Institute. SEER Stat Fact Sheet: Thyroid Cancer. Available at: <http://seer.cancer.gov/statfacts/html/thyro.html>. Accessed October 28, 2013.
3. Thyroid Cancer page. National Cancer Institute, Web site. Available at: <http://www.cancer.gov/cancertopics/types/thyroid>. Accessed January 18, 2010.
4. Lal G, O'Dorisio T, McDougall R, Weigel RJ. Cancer of the Endocrine System. In: Abeloff MD, Armitage JO, Niedernuber JE, Kastan MB, McKenna WG, editors. *Abeloff's Clinical Oncology*. 4th ed. Philadelphia, PA: Churchill Livingstone; 2008. chap 75
5. Prinz RA, Chen E. Thyroid Cancer. In: Bope ET, Rakel RE, Kellerman RD, editors. *Conn's Current Therapy 2010*. Maryland Heights, MO: W. B. Saunders, Elsevier; 2009.
6. Rosove MH, Peddi PF, Glaspy JA. BRAF V600E inhibition in anaplastic thyroid cancer. *N Engl J Med* 2013;368:684-5.
7. Witt RL, Ferris RL, Pribitkin EA, Sherman SI, Steward DL, Nikiforov YE. Diagnosis and management of differentiated thyroid cancer using molecular biology. *Laryngoscope* 2013;123:1059–64.
8. Nikiforova MN, Kimura ET, Gandhi M, Biddinger PW, Knauf JA, Basolo F,

- et al. BRAF mutations in thyroid tumors are restricted to papillary carcinomas and anaplastic or poorly differentiated carcinomas arising from papillary carcinomas. *J Clin Endocrinol Metab* 2003;88:5399-404.
9. Takano T, Ito Y, Hirokawa M, Yoshida H, Miyauchi A. BRAF V600E mutation in anaplastic thyroid carcinomas and their accompanying differentiated carcinomas. *Br J Cancer* 2007;96:1549-53.
 10. Hall RD, Kudchadkar RR. BRAF mutations: signaling, epidemiology, and clinical experience in multiple malignancies. *Cancer Control* 2014;21:221-30.
 11. Chapman PB, Hauschild A, Robert C, Haanen JB, Ascierto P, Larkin J, et al. Improved survival with vemurafenib in melanoma with BRAF V600E mutation. *N Engl J Med* 2011;364:2507-16.
 12. Dietrich S, Glimm H, Andrulis M, von Kalle C, Ho AD, Zenz T. BRAF inhibition in refractory hairy-cell leukemia. *N Engl J Med* 2012;366:2038-40.
 13. Kopetz S, Desai J, Chan E, Hecht JR, O'Dwyer PJ, Lee RJ, et al. PLX4032 in metastatic colorectal cancer patients with mutant BRAF tumors. *J Clin Oncol* 2010;28 Suppl 1:15 (abstr 3534).
 14. Hayes DN, Lucas AS, Tanvetyanon T, Krzyzanowska MK, Chung CH, Murphy BA, et al. Phase II efficacy and pharmacogenomic study of Selumetinib (AZD6244; ARRY-142886) in iodine-131 refractory papillary thyroid carcinoma with or without follicular elements. *Clin Cancer Res*

2012;18:2056–65.

15. Girotti MR, Marais R. Deja Vu: EGF receptors drive resistance to BRAF inhibitors. *Cancer Discov* 2013;3:487-90.
16. Straussman R, Morikawa T, Shee K, Barzily-Rokni M, Qian ZR, Du J, et al. Tumour micro-environment elicits innate resistance to RAF inhibitors through HGF secretion. *Nature* 2012;487:500-4.
17. Corcoran RB, Ebi H, Turke AB, Coffee EM, Nishino M, Cogdill AP, et al. EGFR-mediated re-activation of MAPK signaling contributes to insensitivity of BRAF mutant colorectal cancers to RAF inhibition with vemurafenib. *Cancer Discov* 2012;2:227-35.
18. Cohen Y, Rosenbaum E, Clark DP, Zeiger MA, Umbricht CB, Tufano RP, et al. Mutational analysis of BRAF in fine needle aspiration biopsies of the thyroid: a potential application for the preoperative assessment of thyroid nodules. *Clin Cancer Res* 2004;10:2761–65.
19. Kimura ET, Nikiforova MN, Zhu Z, Knauf JA, Nikiforov YE, Fagin JA. High prevalence of BRAF mutations in thyroid cancer: genetic evidence for constitutive activation of the RET/PTC-RAS-BRAF signaling pathway in papillary thyroid carcinoma. *Cancer Res* 2003;63: 1454–57.
20. Xing M, Tufano RP, Tufaro AP, Basaria S, Ewertz M, Rosenbaum E, et al. Detection of BRAF mutation on fine needle aspiration biopsy specimens: a new diagnostic tool for papillary thyroid cancer. *J Clin Endocrinol Metab* 2004;89: 2867–72.

21. Xing M. BRAF mutation in thyroid cancer. *Endocr Relat Cancer* 2005;12:245-62.
22. Lee J, Hwang JA, Lee EK. Recent progress of genome study for anaplastic thyroid cancer. *Genomics Inform* 2013;11:68-75.
23. Nehs MA, Nucera C, Nagarkatti SS, Sadow PM, Morales-Garcia D, Hodin RA, et al. Late intervention with anti-BRAF(V600E) therapy induces tumor regression in an orthotopic mouse model of human anaplastic thyroid cancer. *Endocrinology* 2012;153:985-94.
24. Montero-Conde C, Ruiz-Llorente S, Dominguez JM, Knauf JA, Viale A, Sherman EJ, et al. Relief of feedback inhibition of HER3 transcription by RAF and MEK inhibitors attenuates their antitumor effects in BRAF-mutant thyroid carcinomas. *Cancer Discov* 2013;3:520-33.

ABSTRACT (IN KOREAN)

BRAF(V600E) 돌연변이 갑상선암에서
BRAF(V600E) 억제에 의한 c-Met 발현 증가가
표적 치료에 대한 저항성 발현에 미치는 영향 분석

< 지도교수 최 은 창 >

연세대학교 대학원 의학과

변 형 권

BRAF(V600E) 돌연변이는 갑상선암에서 가장 흔히 발견되는 유전적인 이상이다. 악성 흑색종에서 보이는 선택적 BRAF 억제제 (PLX4032)의 높은 치료 효과와는 달리, 갑상선암에서의 치료 반응은 낮은 것으로 알려져 있다. 본 연구의 목적은 갑상선암에서 이러한 BRAF 억제제의 낮은 치료 효과의 원인이 되는 내인성 저항 기전을 밝혀 표적 치료의 효과를 극대화하고자 함에 있다. BRAF 돌연변이 갑상선암 세포주에서 BRAF 억제에 따른 피드백 조절 기전의 발현과 상부 신호전달 체계의 변화를 탐색하였다. 또한 이 결과를 바탕으로 하여 병합약물요법에 따른 동시 신호 억제의 효과를 살펴보았다. 두 가지의 갑상선암 세포주인 8505C (역형성 갑상선암)와 BCPAP (유두상 갑상선암)를 선별하여 각각에 대해서 PLX4032를 처리하여 약물의 감수성을 비교 분석하였다. 각각 PLX4032에 대한 상이한 반응의 원인이 되는 신호 변화 양상을 분석하였으며 같은 실험을 정위적 이종이식 마우스 모델에 적용하여 결과를 살펴보았다. BCPAP 세포에서와는 달리 8505C 세포에서는 PLX4032에 대한 약물 저항성을 보였으며, 이는 주로 c-Met의 발현 증가에 기인하였다. BRAF 억제제 (PLX4032)와 c-Met 억제제 (PHA665752)의 동시 투여 후 c-Met, p-AKT, p-ERK 모두 효과적으로 발현이 억제되는 것으로 확인하였으며, 정위적 이종이식 마우스 모델을 이용한 in vivo 동물 실험에서도 유사한 결과를

확인하였다. c-Met을 매개로 한 PI3K/AKT와 MAPK 신호전달 체계의 재활성화가 BRAF 돌연변이 역형성 갑상선암의 PLX4032에 대한 상대적인 약물 저항성에 기여를 하고 있는 것을 확인할 수 있었으며 BRAF와 c-Met의 동시 억제를 통해 지속적인 치료 효과를 얻을 수 있음을 알 수 있었다.



핵심되는 말: BRAF 돌연변이, c-Met, 갑상선암, 표적치료 저항성

PUBLICATION LIST

1. Byeon HK, Na HJ, Yang YJ, Park JH, Kwon HJ, Chang JW, et al. Mechanism of resistance and epithelial to mesenchymal transition of BRAF (V600E) mutation thyroid anaplastic cancer to BRAF (V600E) inhibition through feedback activation of EGFR. Korean J Head Neck Oncol 2014;30:53-61.

